the FEBS Journal

Biochemical and structural analyses of a higher plant photosystem II supercomplex of a photosystem I-less mutant of barley

Consequences of a chronic over-reduction of the plastoquinone pool

Tomas Morosinotto[1,2], Roberto Bassi[1,2], Sara Frigerio[1,2], Giovanni Finazzi[3], Edward Morris[4] and James Barber[5]

1 Université d'Aix-Marseille II, Faculté des Sciences de Luminy, Laboratoire de Génétique et de Biophysique des Plantes (LGBP), CNRS-CEA-Université de la Méditerranée, Marseille, France
2 Dipartimento Scientifico e Tecnologico, Università di Verona, Italy
3 Unité Mixte de Recherche 7141 CNRS, Université Paris 6, Institut de Biologie Physico-Chimique, Paris, France
4 The Institute of Cancer Research, London, UK
5 Wolfson Laboratories, Division of Molecular Biosciences, South Kensington Campus, Imperial College London, UK

Keywords
Lhc; acclimation; photosystem; plastoquinone; supercomplexes

Correspondence
T. Morosinotto, Université d'Aix-Marseille II, Faculté des Sciences de Luminy, Laboratoire de Génétique et de Biophysique des Plantes (LGBP), UMR 6191 CNRS-CEA-Université de la Méditerranée, TPR2, 9ème étage, Bloc 2, 163 Avenue de Luminy, 13288 Marseille Cedex 9, France
Fax: +33 4 91 82 95 66
Tel: +33 4 91 82 95 62
E-mail: morosino@luminy.univ-mrs.fr

(Received 13 July 2006, revised 10 August 2006, accepted 15 August 2006)

doi:10.1111/j.1742-4658.2006.05465.x

Photosystem II of higher plants is a multisubunit transmembrane complex composed of a core moiety and an extensive peripheral antenna system. The number of antenna polypeptides per core complex is modulated following environmental conditions in order to optimize photosynthetic performance. In this study, we used a barley (*Hordeum vulgare*) mutant, *viridis zb63*, which lacks photosystem I, to mimic extreme and chronic overexcitation of photosystem II. The mutation was shown to reduce the photosystem II antenna to a minimal size of about 100 chlorophylls per photosystem II reaction centre, which was not further reducible. The minimal photosystem II unit was analysed by biochemical methods and by electron microscopy, and found to consist of a dimeric photosystem II reaction centre core surrounded by monomeric Lhcb4 (chlorophyll protein 29), Lhcb5 (chlorophyll protein 26) and trimeric light-harvesting complex II antenna proteins. This minimal photosystem II unit forms arrays *in vivo*, possibly to increase the efficiency of energy distribution and provide photoprotection. In wild-type plants, an additional antenna protein, chlorophyll protein 24 (Lhcb6), which is not expressed in *viridis zb63*, is proposed to associate to this minimal unit and stabilize larger antenna systems when needed. The analysis of the mutant also revealed the presence of two distinct signalling pathways activated by excess light absorbed by photosystem II: one, dependent on the redox state of the electron transport chain, is involved in the regulation of antenna size, and the second, more directly linked to the level of photoinhibitory stress perceived by the cell, participates in regulating carotenoid biosynthesis.

Abbreviations
α-DM, n-dodecyl-α-D-maltopyranoside; Chl, chlorophyll; CL, control light; CP, chlorophyll protein; cryo-EM, electron cryomicroscopy; EM, electron microscopy; HL, high light; LHC, light-harvesting complex; LL, low light; NPQ, nonphotochemical quenching; PQ, plastoquinone; PSI, photosystem I; PSII, photosystem II; RC, reaction centre; ROS, reactive oxygen species; VAZ, violaxanthin, antheraxanthin and zeaxanthin.

The energy of solar radiation required to power plant photosynthesis is absorbed and trapped by chlorophyll (Chl) and carotenoids bound to thylakoid membrane proteins, which are organized in two supramolecular complexes: photosystem I (PSI) and photosystem II (PSII). Each photosystem is composed of two moieties with different functions and biogenesis: the reaction centre (RC) core complex, and the peripheral antenna system. In the case of PSII, the RC core complex contains the D1 and D2 subunits, which catalyse electron transport reactions, and Chl proteins (CPs) 43 and 47, which bind Chl *a* and β-carotene. These polypeptides, together with several others contained within the PSII RC core, are encoded by chloroplast genes [1]. The peripheral antenna system of plant PSII is composed of multiple subunits of homologous proteins belonging to the Lhcb (light-harvesting complex) family, which are encoded by nuclear *cab* genes and imported into the chloroplast [2]. They bind Chl *a* and *b* as well as xanthophylls. The size of the peripheral antenna system varies with growth conditions [3–5] and is modulated by the reduction state of the plastoquinone (PQ) pool [6–8] and the accumulation of zeaxanthin, which destabilizes the light-harvesting complex of PSII (LHCII) proteins [9].

The structure of PSII has been the subject of intense research in the past few years, yielding high-resolution maps of the RC core complex isolated from cyanobacteria [10–13] and intermediate-resolution structures for the higher-plant equivalent [14,15]. Crystal structures of the Lhcb proteins that form the trimeric LHCII have also been elucidated to high resolution [16,17]. In contrast, the supramolecular organization of the peripheral antenna system associated with the plant PSII RC core is only known at low resolution, being derived from a combination of electron microscopy (EM), single-particle analyses [18–21] and nearest neighbour analyses [22,23]. Moreover, little is known in structural terms of differences occurring in PSII RC core antenna organization upon acclimation of plants to different light conditions. PSII supercomplexes with a different number of antenna proteins have been observed by EM and single-particle analyses [24], but their presence was not correlated with the physiological state of the plant from which the thylakoid membranes were isolated.

In this work, we studied a barley (*Hordeum vulgare*) mutant, *viridis zb63*, lacking PSI but with normal PSII activity [25]. Because PSI is absent, illumination induces a maximum reduction of the electron flow chain, which is an extreme case of a condition experienced by plants growing in excess light [26]. By subjecting *viridis zb63* plants to different light conditions, we demonstrated that the mutation gives rise to a reduction of the antenna size of PSII to a minimum level that is not further reducible under strong light. As PSII in *viridis zb63* grana membranes has the peculiarity of being organized in two-dimensional arrays [25,27,28], we exploited this characteristic for studying the structural organization of PSII with the minimal antenna. Isolated two-dimensional crystals of PSII from *viridis zb63* were analysed by electron cryomicroscopy (cryo-EM), yielding a projection map at ~20 Å resolution that revealed a dimeric PSII RC core complex surrounded by peripheral Lhc antenna proteins. Biochemical and immunological analyses indicated that the peripheral antenna consists of monomeric Lhcb proteins (CP26, CP29) and trimeric Lhc (LHCII). The LHCII–PSII supercomplex identified in the PSI-less barley mutant is proposed to be the basic structural unit of PSII, with which additional antenna Lhcb proteins associate in wild-type plants in response to the variable environmental conditions.

The analysis of this mutant provides new experimental evidence for the role of the redox state of the PQ pool in regulating the antenna size of PSII by selectively controlling the expression of individual *cab* genes [7,8].

Results

The PQ pool is over-reduced in *viridis zb63*

The *viridis zb63* barley plants carry a mutation causing PSI depletion, which does not affect PSII activity [25]. As this mutation is lethal, the mutant must be propagated in the heterozygous state. Homozygous plants can be distinguished from the wild type by their paler green colour, and can survive for up to 2 weeks on seed reserves, thus allowing chloroplast isolation. Because of the lack of PSI, illumination of *viridis zb63* plants should promote the over-reduction of the photosynthetic electron transport chain. This will bring about an over-reduction of the PQ pool, a condition that can also occur when wild-type plants are exposed to stress conditions, such as high light and/or low temperature. In the mutant, the PQ pool should be over-reduced, as suggested by the observed constitutive phosphorylation of the CP29 subunit [29]. Thus, this mutant is an ideal system in which to test the relationship between changes in light intensity, reduction of the PQ pool, and regulation of PSII antenna size.

Although the hypothesis of a chronic over-reduction of the PQ pool during illumination of a PSI-less mutant is, in principle, reasonable, other mechanisms than electron flow to PSI are also active in the chloroplast [30], and we cannot exclude the possibility that,

at low light intensities, the PQ pool may be partially reoxidized. To test this possibility, we estimated the redox state of the PSII electron acceptors by assessing the *in vivo* fluorescence emission properties of wild-type and mutant leaves exposed to increasing light intensities. Figure 1A shows the light dependency of the PSII quantum yield (Φ_{SII}), a parameter related to the proportion of the light absorbed by PSII [31]. In wild-type leaves, this parameter decreased progressively as light intensity was increased, reflecting the progressive limitation of electron acceptor availability, owing to reduction of the PQ pool. In contrast, PSII efficiency in the mutant showed a steep decrease when the leaves where shifted from dark to light, irrespective of the light intensity employed (Fig. 1A). This implies that the PQ pool in the mutant remains largely reduced under both limiting and saturating light in this strain. Consistent with the absence of sustained light-induced electron flow in the chloroplast, no generation of nonphotochemical quenching (NPQ) (i.e. ΔpH-induced excessive light dissipation) could be detected in *viridis zb63*, in contrast to the wild type. However, PSII is active in the mutant, as evidenced by the finding that the Φ_{PSII} measured in the dark is very similar in dark-adapted leaves (Fig. 1B). In fact, the observed differences probably reflect enhanced fluorescence emission at PSII open centres, owing to some energetic uncoupling between PSII and the free LHCI complexes (see below), rather than the presence of inactive PSII complexes.

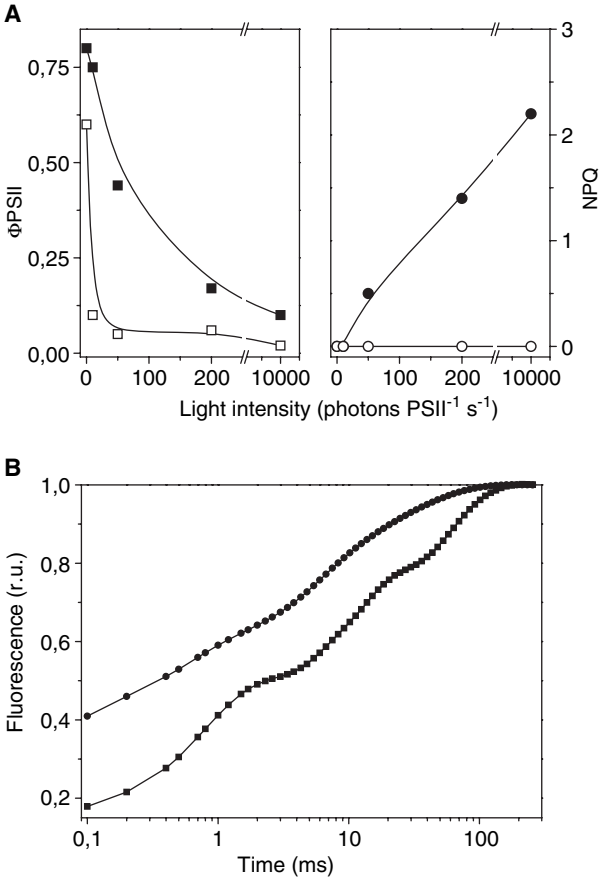

Fig. 1. Determination of the electron transport chain redox state in wild-type (WT) and mutant leaves. (A) Photosystem II (PSII) efficiency (Φ_{PSII}, left panel) was determined by using increasing light intensities in the WT (black squares) and in the mutant (open squares). Nonphotochemical quenching (NPQ, right panel) was also measured; black and white circles represent, respectively, the WT and the mutant. (B) Photosystem II fluorescence induction kinetics in dark-adapted WT (squares) and mutant (circles) leaves.

Antenna size is not regulated in *viridis zb63*

In order to gain more understanding of the relationship between the redox state of the PQ pool and possible changes in PSII antenna size, we subjected the *viridis zb63* barley plants to three different light intensities for 2 weeks: low light (LL = 10 μE), control light (CL = 100 μE) and high light (HL = 1000 μE). As shown above, light differentially affected the redox state of the electron transport chain in the wild type, while promoting a maximum reduction of the chain in the mutant. The different light treatments had an effect on mutant plant phenotype: in HL conditions, plants were paler and survived for 9–10 days only, whereas CL and LL plants survived for up to 14–15 days. LL plants were greener and had ~40% more Chl per unit leaf area with respect to control plants, whereas HL plants had even lower Chl contents. It thus appears that HL and CL treatments cause more extensive damage to the photosynthetic apparatus of the mutant plants than does LL treatment. Thylakoid membranes were isolated from *viridis zb63* plants exposed to the different light treatments, and their pigment composition was analysed. As shown in Table 1, there was a significant reduction in the Chl *b* content of the mutant with respect to the wild type. Although the Chl *a/b* ratio does not provide a precise quantification of the number of Lhcb proteins per PSII core, as Chl *b* is specifically bound to antenna proteins, its relative decrease is an indication of a reduction in antenna size. In the case of wild-type plants, we found that the Chl *b* content was inversely correlated with light intensity, in agreement with many previous reports in a number of species [3–6]: for example, the Chl *a/b* ratio was 3.0 in CL and 3.4 in HL. In contrast, the different light treatments did not appear to have any significant effect on mutant Chl *b* content, suggesting that the PSII antenna size of *viridis zb63* plants was not significantly affected.

Table 1. Pigment composition of wild-type (WT) and *viridis zb63* plants acclimated to different light conditions. The pigment content in thylakoids purified from WT and mutant plants is reported. In the case of the WT, only data from control light (CL) plants are shown. Data are normalized to 100 Chl *a* molecules. The maximum standard deviations determined were 1 for neoxanthin and antheraxanthin, 2 for violaxanthin, zeaxanthin and β-carotene, 3 for lutein and Chl *b*, and 7 for total carotenoid content (Tot Car). LL, low light; HL, high light; VAZ, violaxanthin, antheraxanthin and zeaxanthin.

	Chl *b*	Tot Car	Neoxanthin	Violaxanthin	Antheraxanthin	Lutein	Zeaxanthin	β-Carotene	VAZ
Zb63 CL	19.4	50.4	5.9	4.4	4.4	19.2	7.1	9.3	15.9
Zb63 LL	20.5	50.6	6.4	8.9	1.6	19.4	2.0	12.5	12.4
Zb63 HL	19.3	52.8	5.4	3.8	2.8	17.1	15.5	8.2	22.1
WT CL	31.0	34.6	4.9	5.6	0.0	13.4	0.0	10.8	5.6

In order to confirm that the antenna size is indeed constant in the mutant, we also determined the Lhcb polypeptide content by nondenaturing and denaturing gel electrophoresis. With both techniques, we could not find significant differences in the electrophoretic pattern of thylakoid proteins from mutants grown in different light conditions (SDS/PAGE is reported in Fig. 2A). A third confirmation of the conservation of antenna size in the mutant is provided by the EM experiments reported in detail below: in membranes purified from the mutant, PSII–LHCII supercomplexes have the same size and thus the same number of antenna proteins bound, regardless of the light conditions.

Lack of antenna size acclimation in *viridis zb63* was not due to lack of light stress during the treatment. Indeed, the amount of zeaxanthin, a xanthophyll synthesized only in conditions of excess light [32], was very low in LL plants and very high in HL plants (Table 1). Also, the total amount of carotenoids from the β-branch of the biosynthetic pathway (VAZ, violaxanthin, antheraxanthin and zeaxanthin) increased with illumination intensity. Thus, carotenoid composition in the mutant is modified following the different light treatments, a well-known adaptation to light stress [33,34]. It should be pointed out, however, that in the mutant the stress response appeared at lower light intensities: zeaxanthin and antheraxanthin were

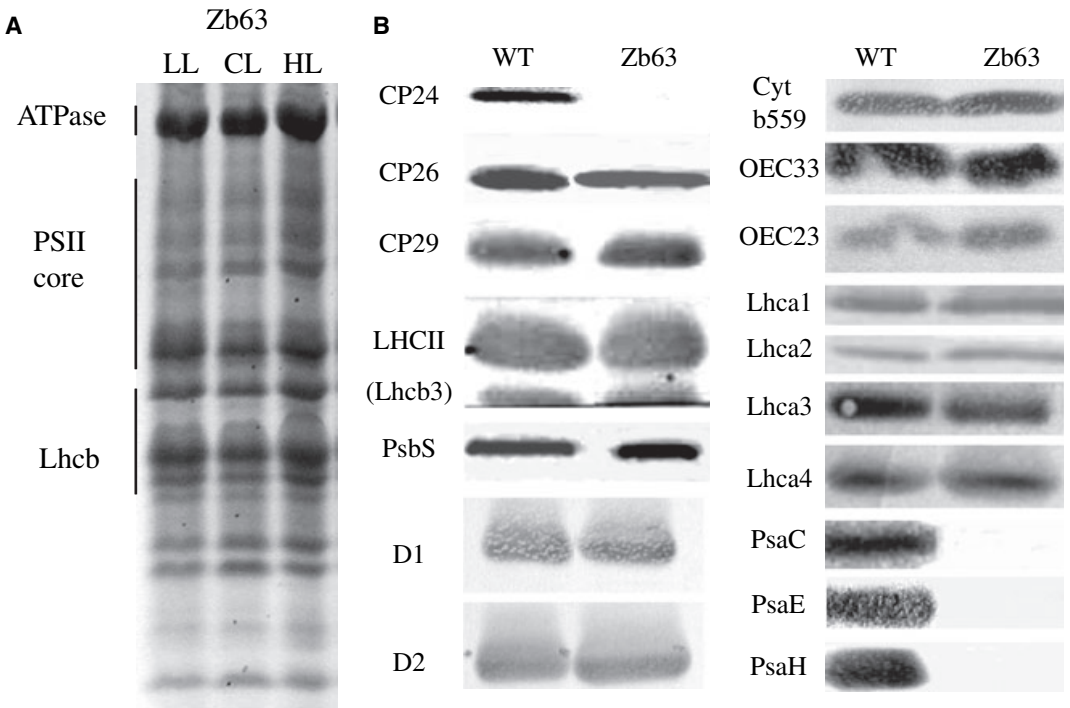

Fig. 2. Protein composition of thylakoid membranes from barley mutant *viridis zb63* (Zb63). (A) SDS/PAGE of thylakoids purified from plants grown under different illumination levels: low light (LL), control light (CL) and high light (HL). Fifteen micrograms of chlorophylls (Chls) were loaded per sample. Band identity, as obtained by western blotting analysis, is also shown. (B) Comparison of polypeptide composition of *viridis zb63 and* barley wild type (WT) grown under control light by immunoblotting.

found in detectable amounts even in LL conditions (2.0 and 1.6 molecules per 100 Chl *a*, respectively), whereas in the wild type they were only found in trace amounts (0.7 molecules per 100 Chl *a*) and only following HL treatment. This indicates that mutant plants experience overexcitation of PSII even when the illumination intensity is very low.

On the basis of these findings, we conclude that the antenna size of the *viridis zb63* mutant does not vary in response to light intensities during growth and increasing degrees of photoinhibition, as found with wild-type plants. Even when the mutant was treated with HL, antenna size was not further reduced: it therefore seems that the *viridis zb63* PSII antenna reached its minimal size, which is not further reducible.

Biochemical analysis of *viridis zb63* thylakoids

In order to characterize the composition of this minimal PSII identified in *viridis zb63*, thylakoids isolated from the mutant were analysed by SDS/PAGE and immunoblotting with antibodies specific for PSI and PSII proteins (Fig. 2B). As expected, PSI core polypeptides (PsaC, PsaE and PsaH) were not detected in the mutant, although the Lhca polypeptides (Lhca1–Lhca4) comprising the LHCI antenna system of PSI were retained. The subunit composition of PSII appears, instead, not to be drastically affected by the mutation in *viridis zb63*: LHCII, CP26 (Lhcb5) and CP29 (Lhcb4) polypeptides are present, and only the peripheral antenna component, CP24 (Lhcb6), is completely absent. Thus, among all the Lhcb polypeptides, only CP24 is not included in the minimal PSII antenna. It should be mentioned that all samples used for blottings were loaded on a Chl basis. Therefore, as Chl content per area is far lower in the mutant (around 20% of that in the wild type in CL), the cellular concentrations of all photosystem polypeptides, including those that appear to be only slightly affected in the mutant, are far lower than in the wild type.

In order to quantify the pigment–protein holocomplexes in the *viridis zb63* mutant as compared to the wild type, thylakoids were solubilized with n-dodecyl-α-D-maltopyranoside (α-DM) and fractionated by sucrose density gradient ultracentrifugation (Fig. 3A). In each case, seven green bands were resolved, albeit in different relative amounts, which were characterized by pigment analysis, absorption spectroscopy and SDS/PAGE and immunoblotting (Fig. 3C). For the *viridis zb63* mutant, the respective bands contained: free pigments (band 1), monomeric antenna proteins (CP26, CP29 and LHCII monomers) (band 2), and trimeric LHCII (band 3), monomeric (band 4) and dimeric (band 5) PSII cores. Bands 6 and 7 contained supramolecular complexes of PSII with Lhcb proteins (Fig. 3C). For the solubilized wild-type thylakoids, the PSI–LHCI holocomplex, absent in *viridis zb63*, migrated in band 5 together with dimeric PSII RC cores and in bands 6 and 7 together with PSII supercomplexes. It is interesting to note that in the mutant, LHCI polypeptides are detected in free Lhc bands, both in monomeric and trimeric bands, as revealed by their distinctive absorption and fluorescence over 700 nm. This migration pattern on sucrose gradients has already been observed in Lhca-depleted plants and was due to the liberation of Lhca dimers [35]. This similarity in migration pattern suggests that LHCI polypeptides are organized as dimers in mutants as well, even in the absence of PSI core.

In Fig. 3B, the chlorophyll distribution among sucrose gradient bands is compared in order to quantify the relative changes in various antenna complexes between the two genotypes. Significant differences are observed upon normalization of the antenna content to the level of PSII cores. In particular, the amount of trimeric LHCII is reduced by a factor of 6, whereas only a small reduction in monomeric Lhcb antennas is found for the mutant relative to the wild type. Thus, the decrease in PSII antenna size in *viridis zb63* is mainly due to a decreased content of trimeric LHCII in addition to the absence of CP24.

Despite this smaller antenna, distinct bands corresponding to LHCII–PSII supercomplexes (bands 6 and 7) are more abundant in *viridis zb63* than in the wild type. This difference is even more striking when we take into account the fact that the corresponding bands derived from wild-type thylakoids also contain significant amounts of LHCI–PSI supercomplex, as judged by the presence of PsaA/B bands in SDS/PAGE analysis (Fig. 3C). Bands 6 and 7 from *viridis zb63* contained the PSII RC core subunits, CP26, CP29 and LHCII, as judged by the SDS/PAGE profile (Fig. 3C) and verified by detection with specific antibodies (not shown).

Structural analysis of PSII supercomplexes

The *viridis zb63* mutant used in this study has been shown to form two-dimensional particle arrays in the thylakoid membranes [25]. Freeze-etching analyses have been conducted on these two-dimensional crystals [25,36], but the method is limited in resolution, due to metal replication of the particle surface. In order to study the structure of the PSII supercomplex of *viridis zb63* with its minimal antenna at a better resolution, a

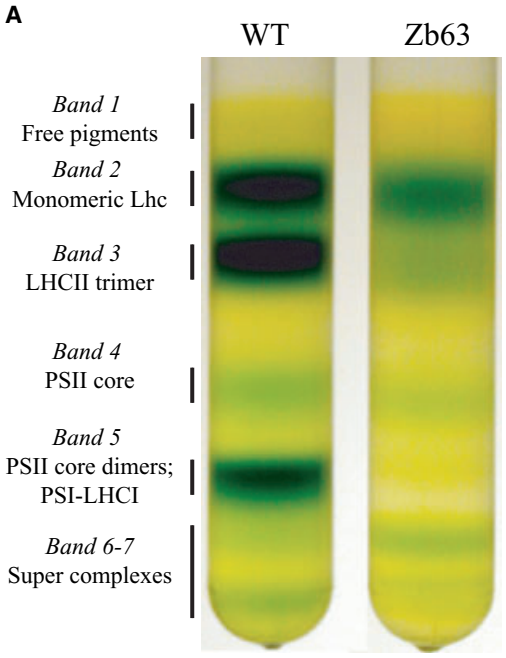

B	% PSII core	
	WT	*zb63*
Band 1	37.4	50.5
Band 2	611.4	484.5
Band 3	864.9	133.0
Band 4	100.0	100.0
Band 5	412.2	14.3
Band 6+7	20.9	89.9
Total	2046.7	872.2

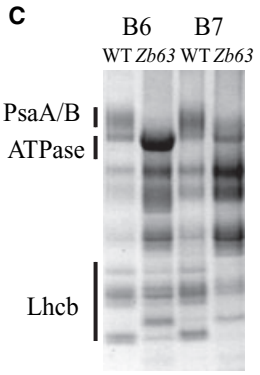

Fig. 3. Separation of pigment-binding complexes by sucrose gradients in wild-type (WT) and mutant plants. (A) Sucrose gradient ultracentrifugation of the WT with *viridis zb63* thylakoids after solubilization with 0.6% n-dodecyl-α-D-maltopyranoside (α-DM). (B) Chlorophyll (Chl) distribution in different sucrose gradients bands of the WT and *viridis zb63*. The quantification of the bands in the two gradients is presented normalized to the photosystem II (PSII) reaction centre (RC) core band. (C) SDS profile of bands 6 and 7 from the WT and mutant (Zb63). Photosystem I (PSI) core major polypeptides (PsaA and PsaB), ATPase subunits and PSII antenna polypeptides (Lhcb) are indicated, as identified by SDS/PAGE analysis.

fractionation treatment was required for selective isolation of ordered grana membranes which are suitable for analysis by transmission EM. Harsh detergent treatment, however, may disturb the regular arrays or modify the crystal spacing with respect to that observed in freeze-fractured membranes [25]. Isolation of grana membranes has been previously performed by fractionation of thylakoids with a limited amount of Triton X-100 [37], yielding two-dimensional crystals of PSII core complexes by selective extraction of peripheral antenna components. More recently, alkyl-glucoside detergents have been employed to isolate PSII supercomplexes containing peripheral antenna systems [18,20,21].

Here we performed a novel separation of grana membranes of *viridis zb63* grown in CL conditions by using different amounts of α-DM in the presence of 5 mM Mg^{2+} to maintain granal stacking [38]. This procedure yielded a membranous fraction that pelleted at 40 000 ***g*** and was depleted in ATPase polypeptides as judged by SDS/PAGE analysis (Fig. 4A). The absence of the ATPase complex indicates that the treatment produced grana membranes free from stroma lamellae. Among a range of detergent concentrations used, 0.1% α-DM allowed the isolation of a pelletable fraction that, upon negative staining, showed roughly circular membrane patches about 0.8 μm in diameter when viewed by EM (Fig. 5A). The size of these patches is consistent with their derivation from whole grana partitions, suggesting that the isolation procedure succeeded in conserving the native state. Consistently, oxygen-evolving activity was maintained after the purification was complete: grana particles from the mutant showed an activity of 561 ± 76 μmol O_2 per mg of Chl per hour, compared to 505 ± 68 measured with the thylakoids. Thus, PSII in the granal membranes is as active in performing its physiological function as PSII in intact thylakoids. In agreement with the mildness of the purification, SDS/PAGE and immunoblotting analyses showed that no major modifications of PSII composition were introduced by the membrane fractionation procedure (Fig. 4B). As shown in Fig. 4B, the amount of PsbS appears to be slightly reduced in grana preparations with respect to thylakoids; however, when it was quantified more precisely by immunotitration, there was no significant difference in content between thylakoids and grana membranes (not shown). A number of PSII-rich patches contained clearly visible, stain-excluding particles arranged in regular rows (Fig. 5A,D). Indexation of Fourier transforms of such images reveal two lattices (Fig. 5B,C). The lattices, which are mirror images of each other, have cell dimensions of 16.5 × 25 nm and lattice angles of 100° or 80°. Images derived by Fourier filtration of each such lattice after appropriate corrections for long-range disorder are characterized by strongly stain-excluding particles (Fig. 5D), consistent with the

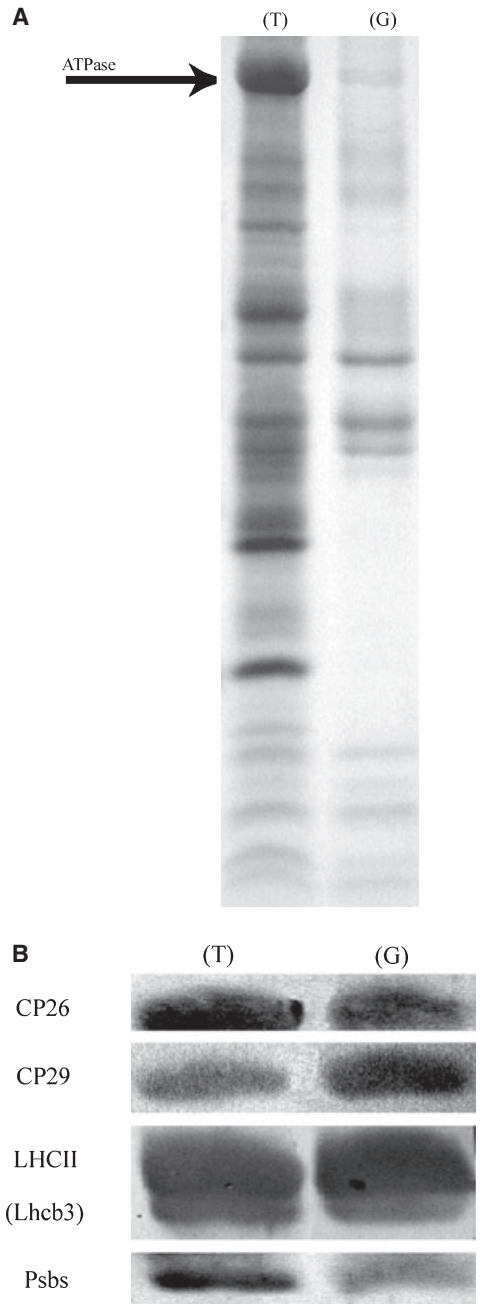

Fig. 4. Analysis of polypeptide composition of grana preparation. Comparison of (A) SDS/PAGE and (B) immunoblotting analyses of the granal membrane preparation (G) isolated from the barley mutant *viridis zb63* used for electron microscopy (EM) studies with its thylakoid membranes (T).

projection appearance of negatively stained dimeric PSII core arrays [14,37,39–41]. The arrangement of the particles within the array is such that they are substantially separated from each other and connected by material that attracts stain much more weakly. This appearance may be explained by the presence of additional protein subunits that do not substantially protrude from the lipid bilayer and are thus only weakly contrasted by negative stain. The spacing of these lattices is consistent with that observed by freeze-fracture of thylakoids [25]. The presence of two mirror-image lattices suggests that the membrane patches consist of two stacked lipid bilayers containing PSII arrays back-to-back.

The data presented above were all obtained with grana membranes isolated from CL-grown mutants. However, when we analysed by EM grana preparations from mutant plants grown in LL and HL conditions, we also found that PSII was organized in arrays. Lattice parameters were also unchanged, thus suggesting that the number of antenna proteins associated with the core complex is maintained, in agreement with the biochemical analyses reported above.

Electron cryomicroscopy and image analysis of the two-dimensional arrays

Preparations from the mutant grown in CL conditions, identified by negative stain as being rich in well-ordered lattices, were subjected to cryo-EM. Patches containing lattices could be recognized with a reasonable success rate at low magnification (4000×) from their size, shape and density. Low-dose images of these patches were recorded at a defocus level of about 0.7 μm. Favourably imaged areas with well-developed crystalline lattices were identified for image analysis. From these regions, Fourier-filtered images were obtained for each of the two component lattices. The filtered images were used as references to obtain the locations of the individual unit cells by cross-correlation. Patches of crystal corresponding approximately to four unit cells were extracted and processed by single-particle analysis methods. In total, 372 patches were aligned and averaged together to produce a projection map (Fig. 6A). The resolution of the map as estimated by the Fourier ring correlation coefficient is about 20 Å (Fig. 6C). Compared to the projection map derived from negatively stained two-dimensional crystals (Fig. 5D), the cryo-EM equivalent shows substantially enhanced structural detail. The central core complex regions contain densities characteristic of projection structures of individual subunits of the PSII core (Fig. 6B) and are connected together by regions of strong density. The particles that make up the array are of a size and shape reminiscent of that of the LHCII–PSII supercomplex studied by single-particle analyses [18,20,21].

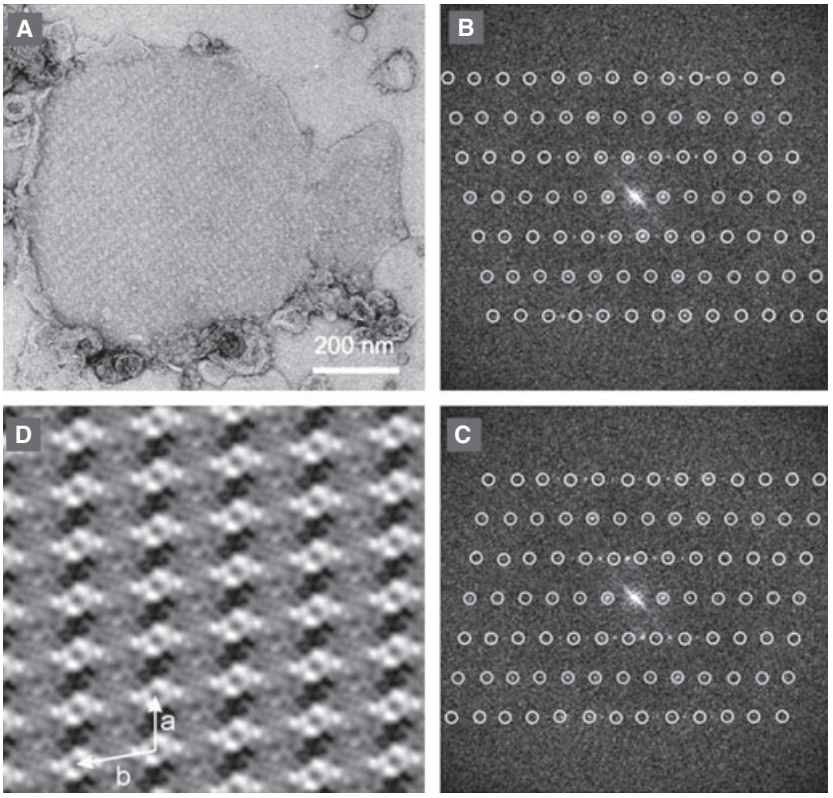

Fig. 5. Characterization of the photosystem II (PSII) supercomplex two-dimensional crystals by EM with negative staining and image analysis. (A) Electronmicrograph of negatively stained two-diemnsional crystal. (B) and (C) Fourier transform derived from (A) displayed as amplitudes. Two reciprocal lattices are identified arising from oppositely orientated PSII supercomplex arrays viewed from the luminal (B) and stromal (C) sides. In both cases, reflections in the second, fourth and sixth rows are common to each reciprocal lattice, whereas the others derive from a single layer. (D) A Fourier-filtered image corresponding to the layer viewed from the lumenal side.

Discussion

The PQ redox state is a key signal for antenna size regulation but not for carotenoid biosynthesis

Acclimation of wild-type plants to increasing light intensities brings about a decrease in the level of LHCII per PSII RC [3–6]. In *viridis zb63*, lacking PSI, we show that the antenna content per PSII RC was already at a minimal level and did not change significantly even at high light intensity. The inability of the *viridis zb63* PSII mutant to adjust its antenna size to different light intensities is confirmed by pigment and polypeptide analysis, which showed the absence of any relevant modification in antenna proteins. In addition, EM of grana particles purified from *viridis zb63* plants grown under different light conditions show that the organization in PSII arrays is maintained. These arrays have the same spacing and cell unit, demonstrating that PSII–LHCII supercomplex size is conserved regardless of growing conditions.

This lack of regulation is probably due to a chronic reduction of the electron transport chain upon illumination, leading to a substantial reduction of the PQ pool even at very low light intensities. We propose, therefore, that the mutant phenotype mimics that of wild-type plants exposed to very strong light. Consistent with this, we show that *viridis zb63* plants exhibit features typical of HL-treated wild-type plants, such as the increase in the xanthophyll pool [33,34] and the accumulation of zeaxanthin [42].

It is known that over-reduction of the PQ pool triggers LHCII degradation [6] and decreases the expression of the encoding *cab* genes [7,8]. In the mutant, we showed that the electron transport chain is over-reduced in the light, even if the illumination level is very low, suggesting that the redox state of the PQ pool, rather than being an indirect effect due to light stress, plays a key role in determining PSII antenna size.

At variance with the changes in the PSII antenna, other phenomena, which are also thought to participate in the photoprotective response, clearly show a light dose–response effect. This is typically the case for zeaxanthin synthesis, and more generally, for the accumulation of the β-branch xanthophyll species (VAZ), which are enhanced at by strong light in both the wild type and *viridis zb63*. This suggests that, although the control of PSII antenna size and the regulation of carotenoid biosynthesis occur in parallel under excess light conditions in wild-type plants, the two processes probably have distinct pathways of activation. Thus, as well as the PQ reduction state, at least one additional signalling

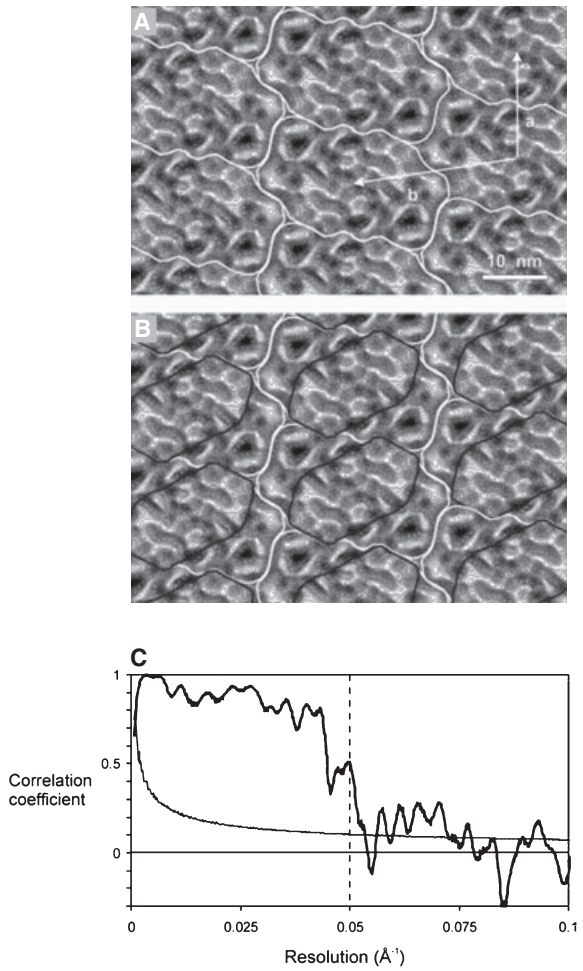

Fig. 6. Projection structure of the photosystem II (PSII) supercomplex array determined by electron cryomicroscopy (cryo-EM) and image analysis. (A) Projection map shown as grey scale overlaid with contours. (B) Projection map as in (A), with the location of the PSII dimeric core outlined in dark grey and the PSII supercomplex outlined in white. (C) Resolution assessment of the projection map by Fourier ring correlation. Correlation coefficient (grey line) and 3σ threshold (black) are plotted as a function of resolution. The approximate resolution of the projection map at 20 Å is shown by a vertical dashed line. Cryo-EM was performed on grana preparations from *viridis zb63* grown under control conditions.

mechanism exists that mediates carotenoid biosynthesis in response to light stress. This signalling pathway appears to respond either directly to light intensity or to its effect on the cell, e.g. reactive oxygen species (ROS) accumulation.

Structural characterization of minimal PSII antenna unit

Our results suggest that the PSII antenna of *viridis zb63* is reduced to the minimal possible level. We characterized this minimal PSII unit using both biochemical and structural methods. When observed by freeze–fracture EM, thylakoids of this mutant show large particle arrays in the grana partition regions, whereas wild-type plants do not [25]. The PSII arrays detected in the grana partitions of *viridis zb63* thylakoids are highly ordered and cover most of the grana membrane surface [28]. Isolation of these particles by Triton X-100 leads to the preparation of paired membranes with opposite orientation, which undergo reorganization and loss of order [37,43]. We have used an alternative method of membrane isolation by employing limited solubilization of stacked thylakoids with the mild detergent α-DM. This procedure produced membrane patches with a diameter of about 0.8 μm, a value comparable to grana dimensions *in vivo* [25]. This correspondence in size suggests that at least some grana remain intact after solubilization. Moreover, this method also yields crystalline patches of paired membranes that do not appear to undergo severe reorganization and can be conserved in a frozen state before structural analysis. The unit cell of these arrays, as identified by negative staining and cryo-EM, was 16.5×25 nm, equivalent to that reported from freeze-etching experiments [28], supporting our view that no major changes were introduced in the organization of the PSII array by the isolation procedure. As PSII in *viridis zb63* has normal activity [27], it is likely that the structural data obtained provide a meaningful representation of functional PSII *in vivo*.

The structures derived from cryo-EM analysis and negative staining clearly show two-fold symmetry (Figs 5D and 6A). The central domain of this dimeric structure, corresponding to the most clearly defined feature in images of negatively stained crystals (Fig. 5D), can be assigned to the dimeric PSII RC core. This assignment is reinforced by the appearance of this domain in the projection map of these crystals derived from cryo-EM. Here, densities can be attributed to secondary structure components within the various subunits of the core complex, as modelled in Fig. 7, consistent with earlier structures of this dimeric core complex of higher plants [14,15,39,41] and with the recent X-ray structure of the PSII core dimer of cyanobacteria [10–12]. Six other masses can be clearly resolved in the structure, symmetrically arranged, with three on each side of the dimeric PSII core domain. Their size and shape correspond to either the trimeric LHCII complex [16] or to its monomeric Lhcb components. The monomeric Lhcb proteins can thus be identified as CP29 (Lhcb4) and CP26 (Lhcb5), due to the absence of CP24 (Lhcb6) in *viridis zb63*. The presence of these monomeric Lhcb proteins and the absence of

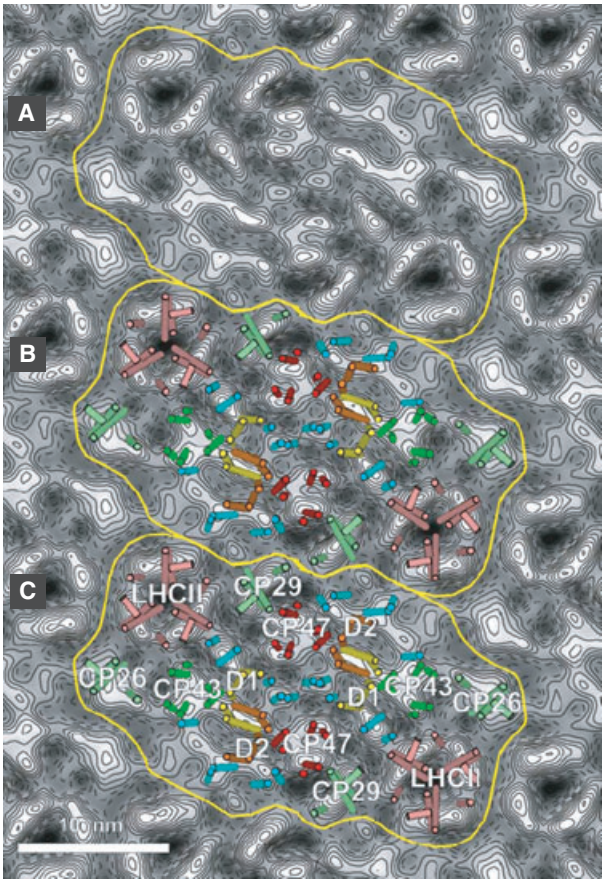

Fig. 7. Interpretation of the photosystem II (PSII) supercomplex projection map. (A) Projection map represented as grey scale with overlaid contours, with PSII supercomplex regions outlined in yellow. (B) Projection map is overlaid with higher-resolution models [15,66], with cylinders representing the transmembrane helices of the plant PSII dimeric core subunits and Lhc subunits. (C) As in (B) with labelled subunits.

CP24 were also found for the isolated PSII–LHCII supercomplex of spinach [44]. Comparison of the molecular structure of the PSII RC core complex [45] with that of the smaller complex lacking the CP43 subunit [46] allowed identification of the CP43 subunit. This earlier assignment has now been confirmed by X-ray crystallography [10–12]. As CP26 forms crosslinking products with CP43 [22], the monomeric Lhcb protein located between the CP43 subunit of the PSII core complex and the trimeric LHCII can be identified as CP26. The remaining mass can therefore be attributed to CP29, which also agrees with the results of crosslinking studies [22] and is supported by EM analysis on single particles [18,20,24]. The above assignments of density to specific subunits within the particle that make up the array in the granal thylakoids of *viridis zb63* are consistent with the assignments previously made for LHCII–PSII supercomplexes isolated from spinach [23,47]. The positions of individual polypeptides in PSII supercomplexes are shown in Fig. 7. Detergent solubilization of the *viridis zb63* thylakoid membranes and the analyses of one of the resulting sucrose density fractions (band 7) confirmed the presence of these LHCII–PSII supercomplexes in the thylakoids of the mutant. The composition of these sucrose density gradient bands was shown to be very similar to that of the granal fraction used for the EM analysis, with a similar Chl *a/b* ratio (6.8 and 6.1, respectively) and a similar SDS/PAGE profile (not shown).

We therefore conclude that the minimal PSII antenna is composed of one trimeric LHCII bound to each side of the PSII RC core dimer through interactions with monomeric CP26 and CP29. It seems that no physiological condition is likely to induce the loss of these peripheral Lhcb antennas, such that the minimal LHCII–PSII supercomplex binds about 100 Chls per PSII RC. The binding of the additional LHCII trimers to this minimal PSII unit provides an outer peripheral system that increases the antenna size to about 250 Chls per PSII RC, typically found in wild-type plants growing under normal conditions.

Differential role of individual Lhcb *cab* genes

The LHCII–PSII supercomplex described above is likely to be present under all environmental conditions. Therefore, it is the association of additional LHCII trimers and CP24 which results in the larger supramolecular organizations (megacomplexes) as visualized by Boekema and colleagues [24]. The formation and adjustment of the outer peripheral LHCII system regulates the absorption cross-section of PSII in response to different growth conditions.

It is interesting to note that CP24 (Lhcb6) is absent in the minimal PSII unit, whereas it is present in wild-type plants grown under normal light conditions [24]. This behaviour suggests a role of this subunit in the regulation of the size of PSII megacomplexes: the presence of CP24 can stabilize the formation of larger complexes, with an extended antenna system, whereas its reduction, in HL conditions, might induce destabilization of the additional antenna subunits, thus inducing a reduction of the antenna size. Therefore, in addition to the light-harvesting function, CP24 may also play an important role in the regulation of antenna size by modulating the stability of PSII megacomplexes. This hypothesis is consistent with the position of CP24 in PSII supercomplexes: in fact, CP24 is found close to LHCII

trimers bound in positions M and L (nomenclature from [24]). In contrast, the trimer composing the minimal antenna unit (S) is bound near CP26 and CP29 but not CP24. It is also interesting to note that *Arabidopsis thaliana* plants acclimated to HL showed a strong reduction of CP24 content [48], consistent with the hypothesis proposed here.

Different Lhcb proteins are found in the peripheral LHCII trimers of PSII megacomplexes than are found within the minimal LHCII–PSII supercomplex. It has already been demonstrated that among Lhcb1, Lhcb2 and Lhcb3 polypeptides, different gene products have distinct properties [49,50] and are expressed differently, depending on growth conditions [51]. It is thus possible that Lhcb1–Lhcb3 polypeptides bound in LHCII trimers of the minimal PSII unit are more effective in photoprotection, whereas those which make up the peripheral LHCIIs are more efficient in light harvesting, in agreement with the proposal that different *cab* gene products play individual roles within the PSII antenna, with a prominent role in light harvesting or photoprotection [52].

The physiological relevance of PSII array formation

It can be asked why these extensive arrays are found in the *viridis zb63* and if such an organization is found only by chance or if it has any biological significance. The former seems unlikely, especially if we consider that similar arrays have been observed in *Arabidopsis* wild-type plants [19,53]. One possible explanation for their presence is that the extensive net of interactions in an array allows more efficient energy transfer among different supercomplexes. Excitation energy is known to equilibrate within grana macrodomains without the need for the presence of PSII arrays. However, such an organization could increase the efficiency of energy equilibration, as approximately 200×10^3 Chls would be in close contact instead of just the 200 Chls of the single PSII–LHCII dimeric supercomplex. Therefore, if light is in excess and the absorbed energy is not trapped by the nearby RC, it can be very efficiently transferred to neighbouring supercomplexes within the array, thus lowering the probability of generation of Chl triplets and ROS. Moreover, in a delocalized system, there is a higher probability of encountering an open RC or a quencher (such as zeaxanthin and/or PsbS [54–56]), whereby excitation energy could be used for photochemistry or safely dissipated as heat. It is worth mentioning that, according to this picture, the hypothetical quencher does not need to be present in one copy per PSII to be effective in photoprotection, and energy could be dissipated relatively far away from the site of light absorption. This possibility is particularly interesting if we consider that the stoichiometry and the localization of PsbS, a PSII subunit fundamental for photoprotection, are still not clear. In fact, an inspection of our projection map for the minimal PSII–LHCII unit indicates that there is not enough space for a four-transmembrane helical protein like PsbS, in accordance with an immunological analysis of the isolated LHCII–PSII supercomplex [21]. Yet, PsbS is present in both *viridis Zb63* and the grana preparation, as shown in Fig. 4B. Thus, if the excitation energy in the system is efficiently delocalized as hypothesized above, PsbS could play its physiological role in spite of a peripheral localization.

It is also interesting to consider how these extensive arrays are generated in *viridis zb63*. In fact, Fig. 3B shows that supercomplexes in the mutants are more abundant and stable with respect to the wild-type plants grown under the same environmental conditions. One factor favouring their formation could be the reduction of the antenna size to the minimum level: this could possibly help the formation of regular arrays, because all PSII particles are uniform in size and composition. Conversely, the presence of the outer LHCII peripheral system in wild-type thylakoids probably prevents the formation of extensive arrays of PSII complexes of the type observed in the grana of *viridis zb63*.

A further factor in the stability of PSII arrays in *viridis zb63* could be the presence of zeaxanthin in the thylakoids. In fact, this xanthophyll was shown *in vitro* to facilitate protein–protein interactions, and it could possibly favour self-organization of PSII into ordered arrays [57].

Experimental procedures

Fluorescence measurements

Fluorescence was measured with a home-built apparatus. Fluorescence was excited using a green LED with a peak emission at 520 nm, and detected in the near infrared. The estimate of the actinic light intensity was obtained by measuring fluorescence-induction kinetics in the presence of saturating concentrations of 3-(3,4-dichlorophenyl)-1,1-dimethylurea (DCMU). We measured the time t at which the variable fluorescence yield was approximately two-thirds of the maximum value. This provides an estimate of the incident photon flux, with a precision of $\pm 10\%$.

Biochemistry

Wild-type and *viridis zb63* plants were normally grown at 100 $\mu E \cdot m^{-2} \cdot s^{-1}$ and 19 °C, with 90% humidity and 8 h of daylight, for 8–10 days. Fluorescence emission was measured using a laboratory-built instrument, as described elsewhere [58]. Thylakoids were isolated as in Bassi *et al.* [59], with the addition of 15 mM NaCl and 5 mM $MgCl_2$ in order to maintain the granal stacking [38]. Thylakoids (0.5 mg $Chl \cdot mL^{-1}$) were solubilized with different amounts of α-DM ranging from 0.05% to 0.75%, always in the presence of 15 mM NaCl and 5 mM $MgCl_2$. Unsolubilized thylakoids were pelleted at 3500 ***g***, and partially solubilized grana membranes were pelleted at 40 000 ***g*** using an SS34 rotor in an RC5C Plus centrifuge from Sorval. Isolated PSII complexes were obtained by extensive solubilization of thylakoid membranes prewashed with 5 mM EDTA in order to remove Mg^{2+}, followed by sucrose density gradient centrifugation as described in Caffarri *et al.* [60]. SDS/PAGE analysis was performed with a Tris/tricine buffer system as in Schägger & von Jagow [61], with an acrylamide concentration gradient of 12–18%. Nondenaturing Deriphat-PAGE was performed following the method developed by Peter & Thornber [62] with the following modifications. The stacking gel had 3.5% (w/v) acrylamide (32 : 1 acrylamide/Bis-acrylamide). The resolving gel had an acrylamide concentration gradient from 4.5% to 11.5% (w/v) stabilized by a glycerol gradient from 8% to 16% (w/v). Tris 12 mM and 48 mM glycine (pH 8.5) were also included in both gels. For analysis by nondenaturing PAGE, thylakoids, at a Chl concentration of 1 $mg \cdot mL^{-1}$, were solubilized with an equal volume of 1.6% α-DM (Anatrace, Maumee, OH), vortexed for 1 min, left for 10 min in ice, and then centrifuged at 13 000 ***g*** in a Microfuge 22R from Beckmann Coulter (Palo Alto, CA, USA) for 15 min for pelleting of unsolubilized material. Thirty micrograms of chlorophylls was loaded per gel lane.

Pigment composition was determined by HPLC analysis [63] and by fitting the acetone extract absorption spectra with those of the individual pigments. Spectra were recorded using an SLM DW 2000 Aminco spectrophotometer (Urbana, IL, USA), in 80% acetone or in 0.5 M sucrose, 10 mM Hepes and 0.06% α-DM.

EM

EM was conducted using an FEI CM200 FEG electron microscope from Phillips (Eindhoven, the Netherlands) operated at 200 kV accelerating voltage in low-dose mode. Images were recorded on Kodak S0163 film at a calibrated magnification of 48 600×. Samples were applied to glow-discharged carbon-coated grids, either stained with 2% uranyl acetate or rapidly frozen by plunging into liquid ethane. Cryo-EM was performed on grana preparations from *viridis zb63* grown in control conditions.

Image analysis

Electronmicrographs were digitized using a Leafscan film scanner from Leaf Systems (Southborough, MA, USA) at a step size of 10 μm. MRC IMAGE programs [64] were used for Fourier space analysis of the two-dimensional crystals, and IMAGIC programs [65] were used in the real space analysis of crystal patches.

Molecular modelling

Molecular models of the spinach core complex [15] and LHCII [66] were superimposed onto the cryo-EM projection map using the program O [67].

Acknowledgements

We would like to thank Professor Diter von Wettstein (Washington State University, Pullman) and Dr David Simpson (Carlsberg Research Laboratory, Copenhagen) for kindly supplying barley wild-type and mutant seeds. This work was supported by Ministero dell'Istruzione dell'Universitá e della Ricerca, Progetto Fondo Investimenti Ricerca di Base (no. RBAU01E3CX) and GENEFUN (functional genetics) program, and the Biotechnology and Biological Research Council (BBSRC) (JB, EM).

References

1 Barber J (2003) Photosystem II: the engine of life. *Q Rev Biophys* **36**, 71–89.
2 Jansson S (1999) A guide to the Lhc genes and their relatives in Arabidopsis. *Trends Plant Sci* **4**, 236–240.
3 Lichtenthaler HK, Kuhn G, Prenzel U & Meier D (1982) Chlorophyll-protein levels and degree of thylakoid stacking in radish chloroplasts from high-light, low-light and bentazon-treated plants. *Physiol Plant* **56**, 183–188.
4 Spangfort M & Andersson B (1989) Subpopulations of the main chlorophyll a/b light-harvesting complex of photosystem II – isolation and biochemical characterization. *Biochim Biophys Acta* **977**, 163–170.
5 Kim JH, Glick RE & Melis A (1993) Dynamics of photosystem stoichiometry adjustment by light quality in chloroplasts. *Plant Physiol* **102**, 181–190.
6 Lindahl M, Yang DH & Andersson B (1995) Regulatory proteolysis of the major light-harvesting chlorophyll a/b protein of photosystem II by a light-induced membrane-associated enzymic system. *Eur J Biochem* **231**, 503–509.
7 Escoubas JM, Lomas M, LaRoche J & Falkowski PG (1995) Light intensity regulation of cab gene transcrip-

tion is signaled by the redox state of the plastoquinone pool. *Proc Natl Acad Sci USA* **92**, 10237–10241.
8 Chen YB, Durnford DG, Koblizek M & Falkowski PG (2004) Plastid regulation of Lhcb1 transcription in the chlorophyte alga Dunaliella tertiolecta. *Plant Physiol* **136**, 3737–3750.
9 Havaux M, Dall'Osto L, Cuine S, Giuliano G & Bassi R (2004) The effect of zeaxanthin as the only xanthophyll on the structure and function of the photosynthetic apparatus in Arabidopsis thaliana. *J Biol Chem* **279**, 13878–13888.
10 Zouni A, Witt HT, Kern J, Fromme P, Krauss N, Saenger W & Orth P (2001) Crystal structure of photosystem II from Synechococcus elongatus at 3.8 A resolution. *Nature* **409**, 739–743.
11 Kamiya N & Shen JR (2003) Crystal structure of oxygen-evolving photosystem II from Thermosynechococcus vulcanus at 3.7-A resolution. *Proc Natl Acad Sci USA* **100**, 98–103.
12 Ferreira KN, Iverson TM, Maghlaoui K, Barber J & Iwata S (2004) Architecture of the photosynthetic oxygen-evolving center. *Science* **303**, 1831–1838.
13 Loll B, Kern J, Saenger W, Zouni A & Biesiadka J (2005) Towards complete cofactor arrangement in the 3.0 A resolution structure of photosystem II. *Nature* **438**, 1040–1044.
14 Morris EP, Hankamer B, Zheleva D, Friso G & Barber J (1997) The three-dimensional structure of a photosystem II core complex determined by electron crystallography. *Structure* **5**, 837–849.
15 Hankamer B, Morris E, Nield J, Gerle C & Barber J (2001) Three-dimensional structure of the photosystem II core dimer of higher plants determined by electron microscopy. *J Struct Biol* **135**, 262–269.
16 Liu Z, Yan H, Wang K, Kuang T, Zhang J, Gui L, An X & Chang W (2004) Crystal structure of spinach major light-harvesting complex at 2.72 A resolution. *Nature* **428**, 287–292.
17 Standfuss J, Terwisscha van Scheltinga AC, Lamborghini M & Kuhlbrandt W (2005) Mechanisms of photoprotection and nonphotochemical quenching in pea light-harvesting complex at 2.5 A resolution. *EMBO J* **24**, 919–928.
18 Boekema EJ, Hankamer B, Bald D, Kruip J, Nield J, Boonstra AF, Barber J & Rögner M (1995) Supramolecular structure of the photosystem II complex from green plants and cyanobacteria. *Proc Natl Acad Sci USA* **92**, 175–179.
19 Boekema EJ, van Breemen JF, van Roon H & Dekker JP (2000) Arrangement of photosystem II supercomplexes in crystalline macrodomains within the thylakoid membrane of green plant chloroplasts. *J Mol Biol* **301**, 1123–1133.
20 Nield J, Orlova EV, Morris EP, Gowen B, van Heel M & Barber J (2000) 3D map of the plant photosystem II supercomplex obtained by cryoelectron microscopy and single particle analysis. *Nat Struct Biol* **7**, 44–47.
21 Nield J, Funk C & Barber J (2000) Supermolecular structure of photosystem II and location of the PsbS protein. *Philos Trans R Soc Lond B Biol Sci* **355**, 1337–1344.
22 Harrer R, Bassi R, Testi MG & Schäfer C (1998) Nearest-neighbor analysis of a photosystem II complex from Marchantia polymorpha L. (liverwort), which contains reaction center and antenna proteins. *Eur J Biochem* **255**, 196–205.
23 Dekker JP & Boekema EJ (2005) Supramolecular organization of thylakoid membrane proteins in green plants. *Biochim Biophys Acta* **1706**, 12–39.
24 Boekema EJ, van Roon H, Calkoen F, Bassi R & Dekker JP (1999) Multiple types of association of photosystem II and its light-harvesting antenna in partially solubilized photosystem II membranes. *Biochemistry* **38**, 2233–2239.
25 Simpson DJ (1983) Freeze–fracture studies on barley plastid membranes. VI. Location of the P700-chlorophyll a-protein 1. *Eur J Cell Biol* **31**, 305–314.
26 Krause GH & Weis E (1991) Chlorophyll fluorescence and photosynthesis: the basics. *Ann Rev Plant Physiol* **42**, 313–349.
27 Hiller RG, Moller BL & Hoyerhansen C (1980) Characterization of 6 putative photosystem-I mutants in barley. *Carlsberg Res Commun* **45**, 315–328.
28 Simpson DJ & von Wettstein D (1980) Macromolecular physiology of plastids. 14. Viridis mutants in barley – genetic, fluoroscopic and ultrastructural characterization. *Carlsberg Res Commun* **45**, 283–314.
29 Bergantino E, Sandona D, Cugini D & Bassi R (1998) The photosystem II subunit CP29 can be phosphorylated in both C3 and C4 plants as suggested by sequence analysis. *Plant Mol Biol* **36**, 11–22.
30 Cournac L, Redding K, Ravenel J, Rumeau D, Josse E-M, Kuntz M & Peltier G (2000) Electron flow between photosystem II and oxygen in chloroplasts of photosystem I-deficient algae is mediated by a quinol oxidase involved in chlororespiration. *J Biol Chem* **275**, 17256–17262.
31 Genty B, Briantais J-M & Baker NR (1989) The relationship between the quantum yield of photosynthetic electron transport and quenching of chlorophyll fluorescence. *Biochim Biophys Acta* **990**, 87–92.
32 Yamamoto HY, Chang JL & Aihara MS (1967) Light-induced interconversion of violaxanthin and zeaxanthin in New Zealand spinach-leaf segments. *Biochim Biophys Acta* **141**, 342–347.
33 Demmig-Adams B & Adams WW (1994) Capacity for energy dissipation in the pigment bed in leaves with different xanthophyll cycle pools. *Aust J Plant Physiol* **21**, 575–588.

34 Davison PA, Hunter CN & Horton P (2002) Overexpression of beta-carotene hydroxylase enhances stress tolerance in Arabidopsis. *Nature* **418**, 203–206.
35 Morosinotto T, Ballottari M, Klimmek F, Jansson S & Bassi R (2005) The association of the antenna system to photosystem I in higher plants. Cooperative interactions stabilize the supramolecular complex and enhance red-shifted spectral forms. *J Biol Chem* **280**, 31050–31058.
36 Miller KR & Jacob JS (1991) Surface structure of the photosystem II complex. In *Proceedings of the 49th EMSA Meeting* (Bailey GW & Hall EL, eds), pp. 196–197. San Francisco Press, San Francisco, CA.
37 Marr KM, McFeeters RL & Lyon MK (1996) Isolation and structural analysis of two-dimensional crystals of photosystem II from Hordeum vulgare viridis zb63. *J Struct Biol* **117**, 86–98.
38 Berthold DA, Babcock GT & Yocum CF (1981) A highly resolved, oxygen-evolving photosystem II preparation from spinach thylakoid membranes. EPR and electron-transport properties. *FEBS Lett* **134**, 231–234.
39 Bassi R, Ghiretti MA, Tognon G, Giacometti GM & Miller KR (1989) Two-dimensional crystals of the photosystem II reaction center complex from higher plants. *Eur J Cell Biol* **50**, 84–93.
40 Santini C, Tidu V, Tognon G, Ghiretti MA & Bassi R (1994) Three-dimensional structure of the higher-plant photosystem II reaction centre and evidence for its dimeric organization in vivo. *Eur J Biochem* **221**, 307–315.
41 Hankamer B, Morris EP & Barber J (1999) Revealing the structure of the oxygen-evolving core dimer of photosystem II by cryoelectron crystallography. *Nat Struct Biol* **6**, 560–564.
42 Demmig-Adams B (1990) Carotenoids and photoprotection in plants: a role for the xanthophyll zeaxanthin. *Biochim Biophys Acta* **1020**, 1–24.
43 Ford RC, Stoylova SS & Holzenburg A (2002) An alternative model for photosystem II/light harvesting complex II in grana membranes based on cryo-electron microscopy studies. *Eur J Biochem* **269**, 326–336.
44 Hankamer B, Nield J, Zheleva D, Boekema E, Jansson S & Barber J (1997) Isolation and biochemical characterisation of monomeric and dimeric photosystem II complexes from spinach and their relevance to the organisation of photosystem II in vivo. *Eur J Biochem* **243**, 422–429.
45 Barber J, Nield J, Morris EP, Zheleva D & Hankamer B (1997) The structure, function and dynamics of photosystem two. *Physiol Plant* **100**, 817–827.
46 Rhee K-H, Morris EP, Barber J & Kühlbrandt W (1998) Three-dimensional structure of the plant photosystem II reaction centre at 8 A resolution. *Nature* **396**, 283–284.
47 Barber J, Nield J, Morris EP & Hankamer B (1999) Subunit positioning in photosystem II revisited. *Trends Biochem Sci* **24**, 43–45.
48 Bailey S, Walters RG, Jansson S & Horton P (2001) Acclimation of Arabidopsis thaliana to the light environment: the existence of separate low light and high light responses. *Planta* **213**, 794–801.
49 Elrad D, Niyogi KK & Grossman AR (2002) A major light-harvesting polypeptide of photosystem II functions in thermal dissipation. *Plant Cell* **14**, 1801–1816.
50 Caffarri S, Croce R, Cattivelli L & Bassi R (2004) A look within LHCII: differential analysis of the Lhcb1–3 complexes building the major trimeric antenna complex of higher-plant photosynthesis. *Biochemistry* **43**, 9467–9476.
51 Caffarri S, Frigerio S, Olivieri E, Righetti PG & Bassi R (2005) Differential accumulation of Lhcb gene products in thylakoid membranes of Zea mays plants grown under contrasting light and temperature conditions. *Proteomics* **5**, 758–768.
52 Horton P & Ruban A (2005) Molecular design of the photosystem II light-harvesting antenna: photosynthesis and photoprotection. *J Exp Bot* **56**, 365–373.
53 Yakushevska AE, Keegstra W, Boekema EJ, Dekker JP, Andersson J, Jansson S, Ruban AV & Horton P (2003) The structure of photosystem II in Arabidopsis: localization of the CP26 and CP29 antenna complexes. *Biochemistry* **42**, 608–613.
54 Li XP, Bjorkman O, Shih C, Grossman AR, Rosenquist M, Jansson S & Niyogi KK (2000) A pigment-binding protein essential for regulation of photosynthetic light harvesting. *Nature* **403**, 391–395.
55 Ma YZ, Holt NE, Li XP, Niyogi KK & Fleming GR (2003) Evidence for direct carotenoid involvement in the regulation of photosynthetic light harvesting. *Proc Natl Acad Sci USA* **100**, 4377–4382.
56 Holt NE, Zigmantas D, Valkunas L, Li XP, Niyogi KK & Fleming GR (2005) Carotenoid cation formation and the regulation of photosynthetic light harvesting. *Science* **307**, 433–436.
57 Ruban AV & Horton P (1999) The xanthophyll cycle modulates the kinetics of nonphotochemical energy dissipation in isolated light-harvesting complexes, intact chloroplasts, and leaves of spinach. *Plant Physiol* **119**, 531–542.
58 Joliot P & Joliot A (2002) Cyclic electron transfer in plant leaf. *Proc Natl Acad Sci USA* **99**, 10209–10214.
59 Bassi R, Rigoni F, Barbato R & Giacometti GM (1988) Light-harvesting chlorophyll a/b proteins (LHCII) populations in phosphorylated membranes. *Biochim Biophys Acta* **936**, 29–38.
60 Caffarri S, Croce R, Breton J & Bassi R (2001) The major antenna complex of photosystem II has a xanthophyll binding site not involved in light harvesting. *J Biol Chem* **276**, 35924–35933.
61 Schägger H & von Jagow G (1987) Tricine-sodium dodecyl sulfate-polyacrylamide gel electrophoresis for the separation of proteins in the range from 1 to 100 kDa. *Anal Biochem* **166**, 368–379.

62 Peter GF & Thornber JP (1991) Biochemical composition and organization of higher plant photosystem II light-harvesting pigment-proteins. *J Biol Chem* **266**, 16745–16754.
63 Gilmore AM & Yamamoto HY (1991) Zeaxanthin formation and energy-dependent fluorescence quenching in pea chloroplasts under artificially mediated linear and cyclic electron transport. *Plant Physiol* **96**, 635–643.
64 Crowther RA, Henderson R & Smith JM (1996) MRC image processing programs. *J Struct Biol* **116**, 9–16.
65 van Heel M, Harauz G, Orlova EV, Schmidt R & Schatz M (1996) A new generation of the IMAGIC image processing system. *J Struct Biol* **116**, 17–24.
66 Kühlbrandt W, Wang DN & Fujiyoshi Y (1994) Atomic model of plant light-harvesting complex by electron crystallography. *Nature* **367**, 614–621.
67 Jones TA, Zou J-Y & Cowan SW (1991) Improved methods for building protein models in electron denity maps and the location of errors in the models. *Acta Crystallogr* **A47**, 110–119.